Matrix Biology xxx (2013) xxx–xxx

Contents lists available at SciVerse ScienceDirect

Matrix Biology

journal homepage: www.elsevier.com/locate/matbio

Effects of decorin proteoglycan on fibrillogenesis, ultrastructure, and mechanics of type I collagen gels

Shawn P. Reese [a], Clayton J. Underwood [a], Jeffrey A. Weiss [a,b,*]

[a] Department of Bioengineering, University of Utah, United States
[b] Department of Orthopedics, University of Utah, United States

ARTICLE INFO

Article history:
Received 13 August 2012
Received in revised form 17 March 2013
Accepted 1 April 2013
Available online xxxx

Keywords:
Decorin
Collagen
Fibrillogenesis
Mechanics
Ultrastructure

ABSTRACT

The proteoglycan decorin is known to affect both the fibrillogenesis and the resulting ultrastructure of in vitro polymerized collagen gels. However, little is known about its effects on mechanical properties. In this study, 3D collagen gels were polymerized into tensile test specimens in the presence of decorin proteoglycan, decorin core protein, or dermatan sulfate (DS). Collagen fibrillogenesis, ultrastructure, and mechanical properties were then quantified using a turbidity assay, 2 forms of microscopy (SEM and confocal), and tensile testing. The presence of decorin proteoglycan or core protein decreased the rate and ultimate turbidity during fibrillogenesis and decreased the number of fibril aggregates (fibers) compared to control gels. The addition of decorin and core protein increased the linear modulus by a factor of 2 compared to controls, while the addition of DS reduced the linear modulus by a factor of 3. Adding decorin after fibrillogenesis had no effect, suggesting that decorin must be present during fibrillogenesis to increase the mechanical properties of the resulting gels. These results show that the inclusion of decorin proteoglycan during fibrillogenesis of type I collagen increases the modulus and tensile strength of resulting collagen gels. The increase in mechanical properties when polymerization occurs in the presence of the decorin proteoglycan is due to a reduction in the aggregation of fibrils into larger order structures such as fibers and fiber bundles.

1. Introduction

Type I collagen is the fundamental building block of connective tissues such as tendon, ligament, skin and bone. It is organized into fibrillar structures via a self-assembly process known as fibrillogenesis, which is to a large extent determined by the intrinsic properties of the collagen molecules themselves. Collagen fibril diameter, length and organization are tightly regulated during fibrillogenesis to produce tissues with different functional properties. For instance, in tendon and ligament, highly aligned collagen fibrils are necessary to facilitate force transmission (Provenzano et al., 2002), while a lamellar organization is necessary in the cornea to maintain transparency (Hassell and Birk). Regulators of fibrillogenesis include fibronectin, other fibrillar collagens (types V and XI), various glycoproteins, and small leucine-rich proteoglycans (SLRPs) (Birk et al., 1990; Svensson et al., 1999; Kadler et al., 2008). The proteoglycans decorin, biglycan, fibromodulin and lumican, are SLRP family members and are believed to play a vital role in guiding the proper assembly of collagen during fibrillogenesis (Scott, 1988; Svensson et al., 1999; Silver et al., 2003; Zhang et al., 2006; Banos et al., 2008). As evidenced by a number of knockout studies in mice, a deficiency in one or more of these proteoglycans (PGs) leads to altered tissue structure and function (Robinson et al., 2005; Zhang et al., 2006).

Of the SLRPs relevant to fibrillogenesis, decorin is arguably one of the most important, and certainly the most well studied (Scott, 1988; Robinson et al., 2005; Zhang et al., 2006; Lujan et al., 2007). Decorin is present in nearly all tissues (Scott, 1988; Kuc and Scott, 1997) and has been implicated in fibrillogenesis and the regulation of certain growth factors such as EGF and TGF-beta (Ruhland et al., 2007). Structurally, decorin consists of a core protein covalently bonded to a highly electronegative dermatan sulfate glycosaminoglycan (GAG). The core protein has a high binding affinity for collagen and is thought to be either a horseshoe- or banana-shaped molecule (Scott and Orford, 1981; Scott, 1996; Scott et al., 2004). The exact 3D conformation of decorin, including whether it functions as a monomer or dimer, remains a subject of debate (Weber et al., 1996; Scott, 2003; Goldoni et al., 2004; Scott et al., 2004). Nonetheless, decorin is almost always found in vivo to be associated with the surface of collagen fibrils (Scott and Orford, 1981; Scott et al., 1981). Decorin proteoglycan and core protein have also been found to bind collagen tightly in vitro, and to localize to collagen fibril surfaces (Brown and Vogel, 1989; Pins et al., 1997; Raspanti et al., 2007; Iwasaki et al., 2008).

Developmental studies have found that increased decorin concentration in tendons of developing mice is concurrent with the lateral and linear growth of fibrils (Zhang et al.), suggesting a role in the regulation of fibril diameter, length and organization. Knockout studies have

* Corresponding author at: Department of Bioengineering, University of Utah, 72 South Central Campus Drive, Rm. 2750, Salt Lake City, UT 84112, United States. Tel.: +1 801 587 7834; fax: +1 801 585 5361.
E-mail address: jeff.weiss@utah.edu (J.A. Weiss).

0945-053X/$ – see front matter © 2013 Elsevier B.V. All rights reserved.
http://dx.doi.org/10.1016/j.matbio.2013.04.004

shown that mice with a decorin deficiency display abnormal fibril structure and organization, as well as fragile tissues with decreased strength and stiffness (Robinson et al., 2005; Zhang et al., 2006). However, in vivo studies make isolating the effects of decorin nearly impossible due to genetic compensation. Thus, in vitro studies have been crucial in the effort to understand the role that decorin plays in the fibrillogenesis of collagen. Decorin inhibits fibrillogenesis in cell-free constructs of polymerized type I collagen (Kuc and Scott, 1997; Douglas et al., 2006), and decorin prevents the aggregation of fibrils into fibers (Raspanti et al., 2007; Iwasaki et al., 2008). There are conflicting reports that decorin regulates the fibril diameter of in vitro collagen constructs (Vogel and Trotter, 1987; Kuc and Scott, 1997; Brightman et al., 2000).

When decorin was originally discovered, its recurring pattern along the surface of collagen fibrils in vivo led to a theory that decorin could bridge or "crosslink" adjacent collagen fibrils via the dermatan sulfate side chain (Scott et al., 1981; Scott and Thomlinson, 1998). Therefore it was hypothesized that decorin contributed to the mechanical properties of tissues such as ligament and tendon via this bridging mechanism. However, our previous research demonstrated that digestion of the DS side chain of decorin had no effect on the mechanical properties of human medial collateral ligament (Lujan et al., 2007, 2009). In contrast, mouse knockout studies identified decorin as a proteoglycan that influences the elastic and viscoelastic tensile behaviors in tendon (Elliott et al., 2003; Robinson et al., 2004a, 2004b). It is possible that these mechanical alterations were due to compensatory or developmental abnormalities intrinsic to decorin-deficient mice, but it is also possible that the decorin core protein is important to the organization of collagen and the associated tissue mechanics. Since the decorin core protein cannot be specifically targeted for enzymatic digestion in tissue, the mechanical contributions of the core protein cannot be examined by ex-vivo mechanical testing.

Collagen fibrillogenesis can be studied in vitro because it is a spontaneous, entropy driven process. In vitro, fibrillogenesis is a two-step process composed of a nucleation phase and a growth phase. The structural integrity of the resulting collagen gel is based on the interaction of physically entangled and fused fibrils, as demonstrated by computational multiscale models of collagen gels (Barocas and Tranquillo, 1997; Chandran and Barocas, 2007; Sander et al., 2009a,b). Although type I collagen fibrillogenesis in vitro is more simplified than the in vivo process since it does not include the same regulatory mechanisms, the fibril nucleation and growth phases are fundamentally the same as that which occurs in vivo, and thus in vitro polymerization provides a convenient model to study the effects of different molecules on fibrillogenesis (Kadler et al., 2008; Kalamajski and Oldberg, 2010). Although studies have examined the in vitro effects of GAGs and decorin on fibrillogenesis and the resulting collagen gel microstructure, the effects on the collagen gel mechanical properties have never been investigated. The purpose of this study was to test whether the presence of decorin during the polymerization of type I collagen gels increases the modulus and tensile strength of the resulting gels. In order to understand the mechanisms by which decorin modifies this mechanical behavior, this study also characterized how the decorin proteoglycan and its individual components (core protein and GAG) affect fibrillogenesis kinetics and the resulting fibrillar organization. This research demonstrates that decorin core protein modulates type I collagen fibrillogenesis in vitro, and results in modified force transmission and mechanical behavior of collagen gels.

2. Results

The inclusion of decorin proteoglycan during the polymerization of type I collagen gels affected the process of fibrillogenesis, the material properties and the fibril organization of the resultant gels. The modulus of the gels increased in a dose dependent manner that was well described by a sigmoidal curve fit (Fig. 1, left panel). The linear modulus was over two times larger for gels containing 50 μg/mL of decorin as compared to control gels (5.8 kPa vs. 2.4 kPa). The tensile strength also increased in a similar fashion (data not shown). The modulus did not increase appreciably from gels with a concentration of 50 μg/mL decorin to gels with a concentration of 100 μg/mL decorin. Decorin also affected the kinetics of fibrillogenesis in a dose-dependent manner, as demonstrated by the turbidity curves (Fig. 1, right panel). The ultimate turbidity and rate of fibrillogenesis (slope of linear region) decreased with an increasing concentration of decorin. The addition of decorin proteoglycan to the gels after polymerization did not change the material properties of the resultant gels (Fig. 2).

To determine the part of the decorin proteoglycan that was responsible for the effects on the mechanical properties of the polymerized gels, decorin core protein and dermatan sulfate were individually polymerized with collagen. Their effects on fibrillogenesis and gel mechanics were then tested. All gels displayed relatively linear stress–strain behavior between 10% and 40% tensile strain, with clear differences in the curves between the groups tested (Fig. 3, upper left). Decorin core protein significantly increased the modulus ($p < 0.001$) and tensile strength ($p < 0.001$) of the gels relative to bovine serum albumin (BSA) control, while DS significantly reduced the modulus ($p < 0.001$) and tensile strength ($p < 0.001$) of the gels relative to the control (Fig. 3, lower left). The modulus and tensile strength of gels

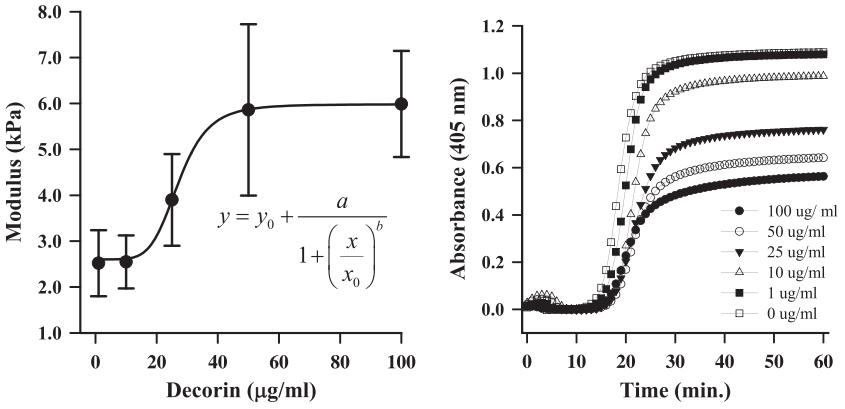

Fig. 1. (Left) The addition of decorin resulted in a dose-dependent increase in the linear modulus of collagen gels. A logistic growth curve provided an excellent fit to the data. Since each data point represents only two samples, the error bars are given to represent the range of the results, not the standard deviation. Curve fit values: $y_o = 2.60$, $x_o = 27.2$, $a = 3.38$, $b = -5.59$. (Right) Decorin changed the kinetics of fibrillogenesis, as demonstrated by the turbidity assay. Increased concentrations of decorin led to increased lag times, decreased rates of fibrillogenesis (slope of linear region) and a decreased ultimate turbidity. (The small absorbance increase at the beginning of all the curves is an artifact of water vapor condensation, as the temperature of the microplate is rapidly changed.) Again, error bars represent the span of the data, not a standard deviation.

Please cite this article as: Reese, S.P., et al., Effects of decorin proteoglycan on fibrillogenesis, ultrastructure, and mechanics of type I collagen gels, Matrix Biol. (2013), http://dx.doi.org/10.1016/j.matbio.2013.04.004

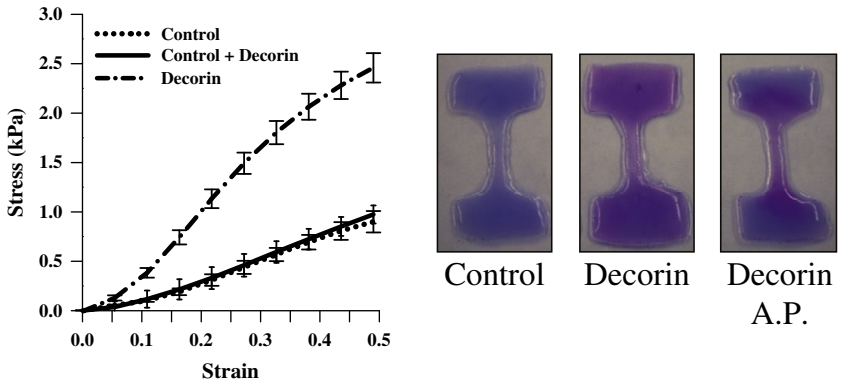

Fig. 2. Timing of decorin addition alters the mechanical properties. (Left) The addition of decorin after the polymerization of the gels did not change the mechanical properties relative to the control. (Right) Gels were washed in PBS and then stained with dimethyl methylene blue which demonstrates the presence of proteoglycan (purple color) within the test region of the decorin polymerized gel and the gel that had decorin added after polymerization (AP). This stain also demonstrated that decorin remains associated with the collagen fibrils and does not diffuse away following polymerization.

polymerized in the presence of the core protein were double that of the control gels, while the modulus and tensile strength of the DS gels were reduced by 1/3 as compared to the control gels. There was no significant difference between the modulus and tensile strength of the decorin and core protein gels. The addition of DS slightly decreased the ultimate turbidity of the gels relative to BSA control, while the core protein and decorin reduced the turbidity, but only decorin PG had a significant effect ($p < 0.05$, Fig. 3, lower right). The decrease in turbidity was greatest with the addition of decorin, followed by the core protein and then DS. There was a significant inverse correlation between the modulus and the ultimate turbidity (Fig. 1, supplemental data).

Since the strain-dependent Poisson's ratio of a fiber network is determined by the fiber network structure (Roeder et al., 2009; Tatlier and Berhan, 2009), the Poisson's ratio of the gels was measured to determine how it was affected by as molecules changed the structure of the fibrillar network. The Poisson's ratio was a nonlinear function of strain for all gels, and it greatly exceeded the isotropic limit of 0.5 (Fig. 3, upper right). The maximum values of the Poisson's ratio were 2.19 ± 0.48 for the decorin gels, 2.60 ± 1.37 for the core protein gels, 1.21 ± 0.24 for the DS gels and 1.91 ± 0.27 for the control gels (Fig. 3, lower left). Only the DS gels had a maximum Poisson's ratio that was significantly different from the control gel ($p < 0.05$). The

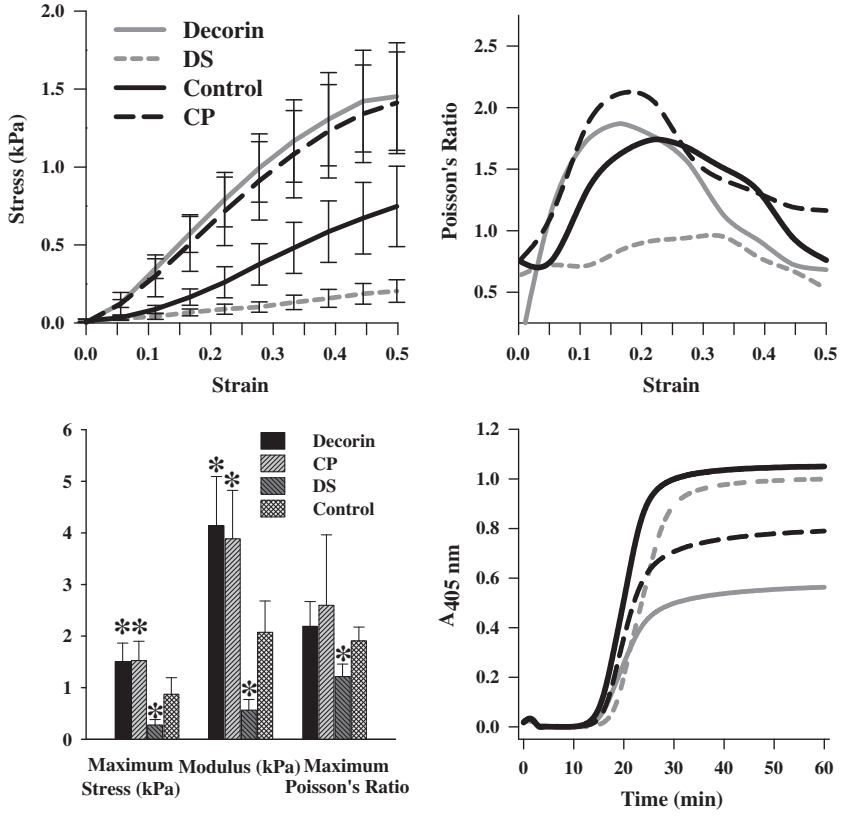

Fig. 3. (Upper left) Stress–strain curves for the collagen gels. Although the stress–strain behavior was nonlinear, a distinct linear region was present. Curves represent mean ± standard deviation. (Upper right) The differential Poisson's ratio was a nonlinear function of strain. Curves represent the average for all samples. Error bars were removed for clarity. (Lower left) The decorin and core protein gels had a higher modulus and tensile strength than the control gels, while the control gels had a higher modulus and tensile strength than the DS gels. The DS gels had a maximum Poisson's ratio that was significantly less than the control gel. Significant differences from control are indicated with asterisks. (Lower right) The ultimate turbidity varied between groups, with decreasing turbidity seen in the DS, decorin core and decorin relative to the control. The lag times also varied, with the DS gels having the largest increase in lag time, followed by the core protein and the decorin gels. Curves represent the average for all samples. Error bars removed for clarity. DS = dermatan sulfate, CP = core protein.

Please cite this article as: Reese, S.P., et al., Effects of decorin proteoglycan on fibrillogenesis, ultrastructure, and mechanics of type I collagen gels, Matrix Biol. (2013), http://dx.doi.org/10.1016/j.matbio.2013.04.004

strain at which the maximum Poisson's ratio was attained varied between the gel groups, but the differences were not statistically significant.

Since decorin proteoglycan and DS changed the mechanical properties of collagen gels in an opposing manner, the fibrillar organization of the resultant gels for each group was examined using SEM. Consistent with previous studies that have examined the structure of collagen gels with SEM and multiphoton microscopy (second harmonic generation) (Brightman et al., 2000; Mosser et al., 2006; Raub et al., 2007; Yang et al., 2009; Bailey et al., 2011), three distinct collagen structures were seen, including single fibrils, fibrils grouped into fibers and fibers grouped into fiber bundles (Fig. 4). This nomenclature, based on previous studies, delineates collagen structures at different length scales (Yang et al., 2009; Bailey et al., 2011). Collagen fibrils, the smallest structure visible in SEM, consist of packed tropocollagen monomers. Fibers, which are formed by the lateral aggregation of fibrils, are visible in both SEM and optical microscopy studies (e.g. confocal reflection microscopy, or CRM). Fiber bundles are the largest structures observed in SEM and CRM and consist of multiple fibers that have laterally aggregated (Yang et al., 2009; Bailey et al., 2011). Qualitative observation indicated that the decorin proteoglycan and core protein gels consisted primarily of either single fibrils or small fibers, while the control gels consisted of both single fibrils and larger fibers. The DS gels consisted primarily of fibers and fiber-bundles.

At a magnification of 15,000× there were noticeable qualitative differences between the SEM images from different groups (Fig. 5, top row). Compared to control, the decorin and core protein gels had denser fibril networks with less grouping of fibrils into fibers. As with the results for material testing, decorin proteoglycan and core protein gels were very similar. Compared to control, the fibrils in the DS gels aggregated more frequently to form a large number of fibers, which often aggregated further into multi-fiber, bundled structures (fiber bundles). Image analysis of SEM images was used to objectively measure the diameter distributions of collagen structures. This analysis revealed that the diameter distributions of collagen structures within the SEM images varied between groups (Fig. 5, bottom row). The computed mean diameter from the SEM images was 78 ± 11 nm for the decorin gels, 84 ± 11 nm for the core protein gels, 125 ± 26 nm for the DS gels and 113 ± 26 nm for the control gels. The mean diameter of both the decorin and core protein gels was significantly different from the control ($p < 0.001$), while the mean diameter of the DS gels was not different. Since SEM only examines the surface structure of dehydrated gels, CRM was also utilized to study the interior of hydrated collagen gels. 60× CRM images revealed similar qualitative observations to that of the SEM. The decorin and core protein gels had collagen structures with a smaller diameter relative to control, while the DS gels had much thicker and shorter collagen structures as compared to the control (Fig. 5, middle row). Image analysis was used to objectively quantify the diameter of collagen structures within the CRM images. The image analysis algorithm revealed that the decorin and core protein gels had distributions with smaller diameters relative to control, while the DS gels had a distribution with larger diameters. The mean structure diameter from the confocal images was 883 ± 13 nm for the decorin gels, 888 ± 20 nm for the core protein gels, 1090 ± 43 nm for the DS gels and 965 ± 40 nm for the control gels. The mean diameter for the decorin and core protein gels was significantly less than the control ($p < 0.001$), while the mean diameter was significantly larger for the DS gels relative to control ($p < 0.001$). In addition, the area occupied by collagen structures (% coverage) was significantly greater in the decorin containing gels ($p < 0.001$), and significantly less in the DS-containing gels ($p < 0.001$).

In the absence of decorin, gels polymerized at 37 °C had a stiffness that was nearly double that of the room temperature (RT) control. In the presence of decorin, gels polymerized at 37 °C were nearly 4 times stiffer than the RT control and twice as stiff as the 37 °C control (Fig. 6). SEM imaging revealed that the control gels polymerized at 37 °C had dense networks primarily consisting of single fibrils. The network topology of the decorin gels polymerized at RT and 37 °C was indistinguishable from the control gels polymerized at 37 °C (data not shown).

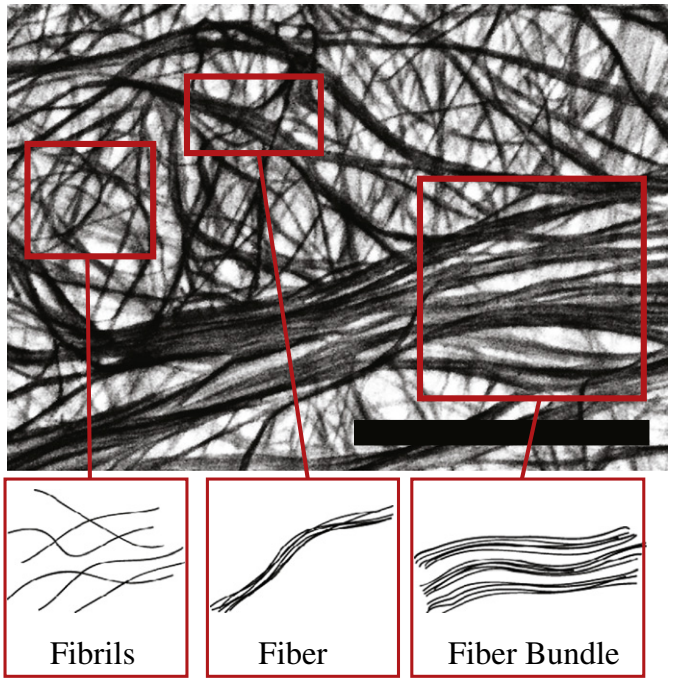

Fig. 4. Top — A 5000× SEM image of a 2 mg/mL control gel (polymerized at RT) demonstrates the three different collagen structures observed within the gels. These include single *fibrils* (left), multiple fibrils grouped into *fibers* (middle) and multiple fibers grouped into *fiber bundles* (right). Image has been inverted so that the fibrils and fibers appear black. Black scale bar = 5 μm.

3. Discussion

This study demonstrated that the presence of decorin during polymerization of type I collagen significantly increased the modulus and tensile strength of the resulting gels. We hypothesize that the mechanism by which decorin increases the mechanical strength of the gels is through modification of collagen fibril organization during fibrillogenesis. This is evidenced by the significant decrease in the mean collagen structure diameter (fibril and fiber diameter) induced by the presence of decorin during polymerization. This correlation is consistent with previous observations, which found that decreased fiber diameter was associated with increased gel strength in collagen gels (Roeder et al., 2002; Raub et al., 2007). It has been suggested that decreased fiber diameters result in a network with increased interconnectedness, thus facilitating more efficient force transfer (Roeder et al., 2009). In thermoreversible 3D crosslinked networks with a liquid organic phase, increasing the junction density (i.e. number of fiber connections) increased the storage modulus (Shi et al., 2009). Our measurements of the area occupied by collagen structures using CRM revealed that decorin-containing gels had a greater area than control or DS-containing gels. This is in agreement with the results of a previous study, which reported that decorin significantly increased the cross-sectional area of fibril-occupied space (Iwasaki et al., 2008). Taken together with the results of the present study, the presence of decorin during fibrillogenesis appears to increase the mechanical properties of collagen gels by preventing the lateral aggregation of fibrils into higher order structures, which in turn may promote longer fibrils that are more interconnected, resulting in a stronger collagen gel.

Please cite this article as: Reese, S.P., et al., Effects of decorin proteoglycan on fibrillogenesis, ultrastructure, and mechanics of type I collagen gels, Matrix Biol. (2013), http://dx.doi.org/10.1016/j.matbio.2013.04.004

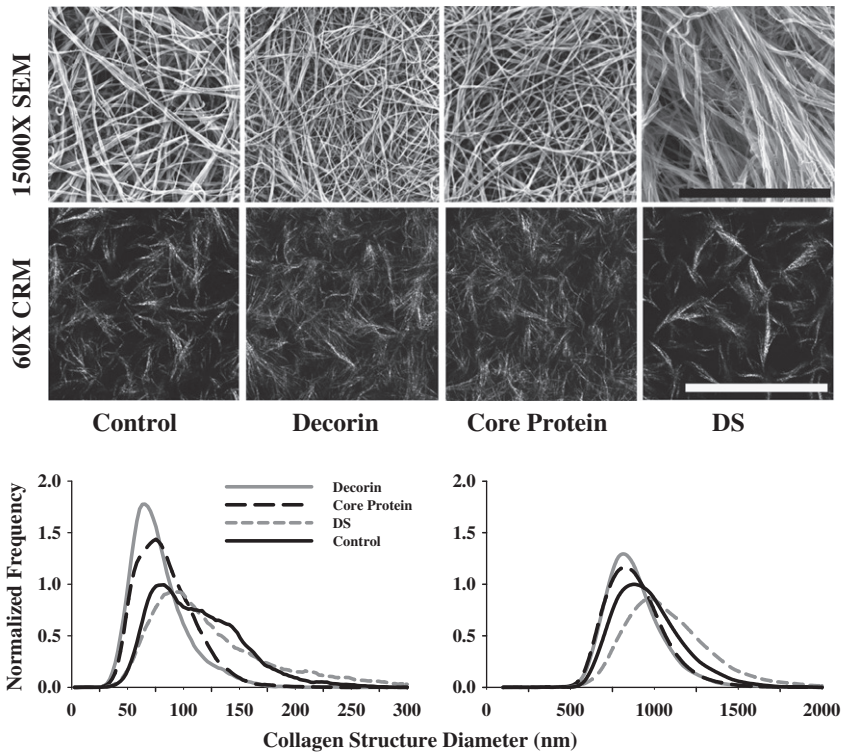

Fig. 5. Top row: Representative 15,000× SEM images are shown for the control (left), decorin (center left), core protein (center right) and DS (right) gel samples. Black scale bars = 5 μm. Center row: Representative 60× confocal images are shown for the control (left), decorin (center left), core protein (center right) and DS (right) gel samples. White scale bar = 75 μm. Bottom row: The normalized collagen structure diameter distributions for the 15,000× images (left) reveal a significant difference in structure diameter for the decorin and core protein gels as compared to the control and DS gels. The collagen structure diameter distribution for the confocal images (right) reveals a significant difference for the structure diameter between the decorin, core protein and DS gels relative to the control. All distributions were normalized relative to the control.

Alternative mechanisms that could explain the increased mechanical strength of the decorin gels include the presence of more end-to-end fibril fusions (Cheema et al., 2007), a change in mean fibril length (Craig et al., 1989), or an altered mean fibril diameter (Silver et al., 2003). Unfortunately, SEM imaging does not allow for the direct measurement of fibril length or the observation of end-to-end fibril fusions, as tracking single fibrils is not possible given the overlap that results from gel dehydration. Although serial sectioning combined with transmission electron microscopy has been used (Birk et al., 1989, 1997; Zhang et al., 2005), tracking the length of fibrils and end-to-end fibril fusions primarily yields qualitative data. Thus, to allow the investigation of these other possible mechanisms, alternative quantitative imaging techniques will be needed to reconstruct multiple 3D image fields of fibrils.

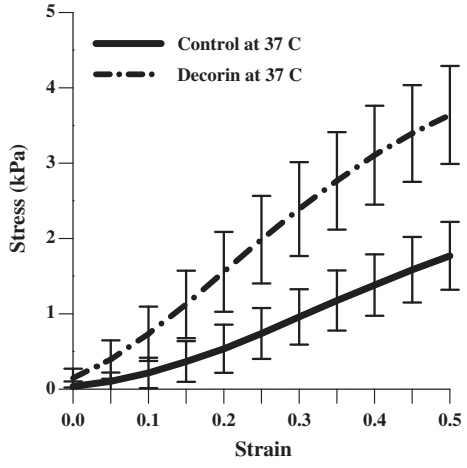

Fig. 6. Effects of increased temperature on polymerization. Increasing temperature to 37 °C did not change the observation that the addition of decorin prior to polymerization leads to increased gel strength. As evidenced by the stress–strain curves, polymerization at 37 °C resulted in decorin gels with a stiffness and tensile strength that was approximately double that of the control.

The addition of the DS side chain of decorin during the polymerization of collagen increased the aggregation of fibrils into fibers and the aggregation of fibers into fiber bundles. This change in fiber organization ultimately led to a significant decrease in linear modulus and tensile strength of the gels. Whereas the decorin core protein increased the gel stiffness by decreasing the fiber diameter, the DS decreased the stiffness by increasing the fiber diameter. This is very interesting considering that when an equivalent amount of DS was added as part of the intact decorin proteoglycan to gels, this effect was not observed. This suggests that DS may be localized differently, or held in a different conformation when attached to decorin. However, a recent study suggests that DS localizes to the same D-period of collagen fibrils whether the core protein is present or absent (Raspanti et al., 2008). It is also possible that there are compositional differences between DS from intestinal mucosa and tendon. We hypothesize that this is a result of decreased fiber connectivity, and thus reduced force transfer through the fiber network. This reduced connectivity and the reduced area occupied by fibrils/fibers can be easily seen in the confocal images of the DS gels (Fig. 4).

The results of our in vitro studies do not support the hypothesis that decorin contributes directly to the material properties of connective tissues by bridging adjacent collagen fibrils and thus transferring force between fibrils. In the present study, decorin had to be present during fibrillogenesis to enhance the material properties of the gels, and when decorin was added after fibrillogenesis, it had no effect. If decorin was responsible for transferring forces between fibrillar structures in gels, the addition of decorin after polymerization would yield similar results as that added before polymerization. Also, it was found that the core protein facilitates a similar increase in mechanical

Please cite this article as: Reese, S.P., et al., Effects of decorin proteoglycan on fibrillogenesis, ultrastructure, and mechanics of type I collagen gels, Matrix Biol. (2013), http://dx.doi.org/10.1016/j.matbio.2013.04.004

strength to that of the whole decorin molecule. This again rules out the possibility of a mechanical contribution from direct interaction of the DS GAG chains, which was integral to the fibril bridging hypothesis and model. Although it is still possible that the decorin PG bridges between fibrils, based on the results of the present study and our previous studies on selective enzymatic degradation of DS in intact ligaments (Lujan et al., 2007, 2009), the mechanism must be independent of the GAG side chain.

The results of this study suggest a possible role for decorin in vivo, namely that its primary function during fibrillogenesis is to prevent the aggregation of fibrils. According to proposed morphogenesis models (Banos et al., 2008), small diameter, immature fibrils fuse to form larger diameter, mature fibrils. By preventing the aggregation of fibrils, decorin would act to prevent further lateral growth of fibrils. This is consistent with the experimental observation that a decorin deficiency leads to abnormally large fibrils during development (Danielson et al., 1997; Zhang et al., 2006, 2009).

The Poisson's ratios reported in this study provide information regarding the structure of the fiber network and load transfer within the network (Tatlier and Berhan, 2009). Previous studies in collagen found that decreased Poisson's ratios were associated with larger fibers and less fiber connectivity (Roeder et al., 2009). In the present study, the DS gels had larger fibers, less area coverage in the CRM images and lower Poisson's ratios, which is consistent with this observation. The nonlinear shape of the Poisson's ratio versus strain curve (Fig. 3) is a result of increasing fiber recruitment, and the shape is similar to that predicted for random fiber networks (Ateshian et al., 2009). According to analytical models, maximal Poisson's ratios will occur at a critical strain during the alignment of the initially random network, and will decrease as fibers became more aligned. This is consistent with multiscale modeling studies that found progressive alignment of the collagen networks under strain (Sander et al., 2009b). Taken together, these results indicate that the material behavior of the collagen gels is consistent with that of random fiber networks. Since the maximal Poisson's ratios were similar between the control and decorin gels, this implies that the two groups of gels had similar organization of the fiber networks. This suggests that the increased fiber diameter is the source of the lowered mechanical strength, rather than an alteration to the network organization. Although the network organization is similar, larger fibers may result in fewer network connections and a net decrease in force transmission, thus resulting in lower strength but unmodified Poisson's ratios.

This is the first study to simultaneously examine the effects of the decorin proteoglycan on fibrillogenesis, collagen gel structure and mechanical properties. Thus, direct comparison of our findings to other studies can be performed, but only on a limited basis. Only a single study has examined the effects of decorin on the tensile properties of collagen (Pins et al., 1997). This study saw a 1.8-fold increase in the linear modulus when decorin was added. However, due to the large variability in their system, there was not a statistical significance when compared to the appropriate control. That study tested extruded collagen fibers that were dried prior to mechanical testing, which changes the material properties of collagen. In a similar study, a synthesized decorin like peptidoglycan (DS-SILY) increased the tensile strength but not the modulus of electrochemically aligned collagen threads (Kishore et al., 2011). Since the decorin proteoglycan itself was not used, the results of this study may not accurately model in vivo behavior. Several studies have examined the effects of decorin on collagen fibrillogenesis using the turbidity assay (Vogel et al., 1984; Vogel and Trotter, 1987; Uldbjerg and Danielsen, 1988), and most reported that decorin decreases ultimate turbidity, although some studies reported no change or an increase in turbidity. A decrease in turbidity has been directly attributed to smaller diameter collagen structures (Kaya et al., 2005).

Previous studies have reported that decorin modifies the grouping of fibrils into fibers (Raspanti et al., 2007; Iwasaki et al., 2008). It was suggested that decorin prevented side-to-side fibril aggregation. A structural study suggested that decorin may preferentially bind to whole fibrils, pointing to a regulatory role for decorin at the fibril level (Orgel et al., 2006). Numerous studies have shown that the decorin core protein binds to type I collagen fibrils within the D period, possibly via two separate binding domains (Pringle and Dodd, 1990; Fleischmajer et al., 1991; Hedbom and Heinegard, 1993; Rada et al., 1993; Schonherr et al., 1995). It is thought that the binding of the core protein may act as a "cap" in order to prevent lateral growth or fibril fusions. Interestingly, the decrease in collagen structure diameter resulting from the addition of decorin in the present study (Fig. 5) is similar to the decrease in diameter seen from increasing the temperature during polymerization (Roeder et al., 2002). We found that the increase in mechanical strength and decrease in structure diameter was similar between decorin gels polymerized at room temperature and control gels polymerized at 37 °C. The mechanism by which this occurs is still under investigation.

The ratio of the ratio of tropocollagen to decorin in this study was slightly lower than that observed in native tendon and ligament. We used a ratio of 4.9:1 (assuming a molecular weight of 300 kDa for tropocollagen and 100 kDa for decorin). In native tendon and ligament tissue, the concentration of decorin is ~1% by dry weight (Kjaer, 2004), which equates to a molar ratio of collagen to decorin of 33:1. However, in native tissue, fibril diameters are larger than in collagen gels. Since decorin localizes to the outside of the fibril, it is expected that a lower molar ratio of collagen to decorin would be needed in the case of smaller diameter fibrils.

Several parameters have been shown to affect the diameter of collagen fibrils/fibers during in vitro fibrillogenesis, including temperature, pH, collagen concentration, and the addition of various molecules (Roeder et al., 2002; Raub et al., 2007). In addition to the effects of decorin core protein and DS GAG on collagen gel microstructure seen in the present study and reported by others (Raspanti et al., 2007; Iwasaki et al., 2008), other glycoproteins and SLRPs such as fibromodulin are known to regulate fibrillogenesis or fibril diameter in vitro and in vivo (Hedbom and Heinegard, 1989; Svensson et al., 1999). Type V and XI collagens both can facilitate the nucleation step of fibrillogenesis in vivo (Wenstrup et al., 2011). Heterotypic mixtures of type V and type I collagen also lead to fibril populations with decreased diameters (Birk et al., 1990). Based on the results of the present study, it is expected that both fibromodulin and collagens type V or XI would also increase the mechanical properties of type I collagen gels, since they decrease fibril diameter.

One of the challenges in the current study was the automated measurement of the multiscale fibril organization. Three types of collagen structures were observed: single fibrils, fibril aggregates (which were termed fibers) and fiber bundles. It is important to emphasize that the term fiber in this context is not synonymous with the use of the term in native connective tissues (e.g. tendon), as native fibers have considerably larger diameters. Attempts at manually quantifying these structures resulted in data of high variability, as distinguishing the difference between two adjacent fibrils and a fiber was subjective. In order to remove this ambiguity from the data, an automated image analysis algorithm was used to quantify the diameter of collagen structures. This algorithm used an automated thresholding scheme which combined fibrils and fibers that were adequately close into a single structure, providing a consistent method for determining the diameter distribution of collagen structures. Since the algorithm identified the general collagen structure diameter, it did not distinguish between fibrils, fibers and fiber bundles. In the SEM images, fiber bundles were often not recognized, as fibers within a bundle may not have been adequately closed to be combined by the thresholding algorithm. Therefore, the automated analysis of the SEM images was able to accurately quantify fibril and fiber structure diameters, but not fiber bundle structure diameters.

Interestingly, image analysis of the CRM images was able to quantify fiber bundle diameters. This is a result of the fact that the inter-fiber spacing in the bundles was too small to be resolved due to the diffraction

Please cite this article as: Reese, S.P., et al., Effects of decorin proteoglycan on fibrillogenesis, ultrastructure, and mechanics of type I collagen gels, Matrix Biol. (2013), http://dx.doi.org/10.1016/j.matbio.2013.04.004

limit of light. Thus, fiber bundles appeared as single structures in the CRM images, resulting in distinctly different diameter distributions between the control and DS gels, which were not seen in the SEM image analysis. It was found that the 15,000× images were most useful for resolving the fine scale differences between the decorin, core protein and control gels, while the 60× CRM images were most useful for resolving the differences between the DS and control gels. This highlights the importance of observing the fiber structure at multiple levels of magnification, as the regulation fibrillogenesis is clearly multiscale. Also noteworthy was a shift in magnitude of the fiber diameters between SEM and CRM, as previously described by Raub et al. (2007). CRM diameters were approximately an order of magnitude larger than that of SEM. This increase in diameter has been ascribed to the hydration of fibrils observed with CRM, and the dehydrated fibrils observed using SEM.

In conclusion, the decorin proteoglycan and the decorin core protein increase the modulus and tensile strength of collagen gels when present during polymerization, and this effect appears to be due to inhibition of fibril aggregation. In addition to clarifying the fundamental role of decorin in modulating collagen fibrillogenesis, this result may provide an approach to increase (or decrease in the case of addition of DS) the material properties of collagen gels, which has relevance to the area of tissue engineering. Collagen and other types of hydrogels have been utilized as medium to deliver cells and other soluble factors to diseased or injured tissues. Inclusion of decorin within these constructs could possibly serve two functions: 1) increasing the strength of the constructs to better withstand surgical manipulation or in vivo mechanical forces and 2) the DS side chain of decorin can act as a reservoir for growth factors (Ruhland et al., 2007) exogenously added or secreted by implanted cells.

4. Methods

4.1. Decorin purification

Decorin was originally obtained from a commercial resource (D8428, Sigma) as cited in previous studies (Pins et al., 1997; Iwasaki et al., 2008), but it was found to be contaminated with approximately 50% biglycan, another SLRP (Supplement Fig. 2, lanes 1 and 2). To ensure that the results of the experiments described were due to decorin and not biglycan, decorin was purified from bovine tendon (Danielson et al., 1997). Purified decorin proteoglycan and the protein core following treatment with chondroitinase ABC treatment are shown in Supplemental Fig. 2 (lanes 3 and 4 respectively). The absorbance of decorin solutions at 280 nm was used to calculate the protein concentration using an extinction coefficient of 19,285 M^{-1} cm^{-1}. The concentration of GAG in the decorin solution was also determined, using the dimethyl methylene blue (DMB) assay (Farndale et al., 1986).

4.2. Gel preparation

Type I collagen gels (2 mg/mL, rat tail, BD Biosciences) were prepared for fibrillogenesis assays and mechanical gel testing. Collagen solutions were mixed on ice, with the reagents added in the following order: collagen, H_2O, test molecules (decorin, dermatan sulfate, etc. in 1× PBS), 10× PBS containing phenol red, and 1 N NaOH. One mL of solution was pipetted into dog-bone shaped silicone molds (40 mL × 20 mL × 1 mL, gauge length = 20 mm), which were pressed onto glass plates (Roeder et al., 2002). Immediately after pouring, four black microbeads (300 μm) were placed on the surface to act as markers for tracking strain during testing. Gels were polymerized at room temperature unless stated otherwise. Room temperature was chosen so that the results could be compared to those of previous studies (Roeder et al., 2002, 2009). 150 μL of the solution was also pipetted in duplicate into 96 well plates for monitoring fibrillogenesis. Changes in turbidity (or light scattering) at a wavelength of 405 nm were monitored over time and used to quantify the kinetics of fibrillogenesis including rate, ultimate turbidity and lag time.

4.3. Material testing

A mechanical testing system was assembled following a previous study. Briefly, it consisted of a movable linear stage, a 10 g load cell (resolution ± 0.005 g), an acrylic test chamber and two plastic clamps for gripping the sample (Supplemental Fig. 3). Two cameras (Allied Vision, 1360 × 1024 pixels) were placed above and to the side of the test chamber to measure the sample cross section and to track strain. Two white LED lamps were placed at an angle to illuminate the sample. Stage movement, data acquisition and video acquisition were controlled via a PC. The stage and data acquisition were controlled using Aerotech A3200 software (Aerotech Inc., Pittsburgh, PA) and the image acquisition was controlled using the DMAS 6 software (Spica Technology Corp, Kihei, Maui). The acrylic chamber was filled with room temperature PBS prior to testing.

Samples were polymerized in groups of twelve and mechanically tested the following day, with each group consisting of 3 gels from each of the four test conditions. The groups (described in more detail in Section 4.8) consisted of a gel polymerized in the presence of bovine serum albumin (BSA) as control, decorin proteoglycan, the decorin core protein and the DS GAG side chain. A total of three groups of twelve were tested, giving a sample of N = 9 for each group. Dehydration was prevented by placing the gels in a humidified chamber consisting of a Nunc Bioassay dish (245 × 245 × 25 mm) with moistened Kimwipes sealed inside. The material properties of the gels stabilized approximately 16 h following the onset of polymerization (Roeder et al., 2002). Samples were removed from the molds, attached to the tissue clamps and secured using nylon screws. The gels were then subjected to constant strain rate testing at 10 mm/min (~0.8%/s) until failure. This strain rate was chosen so that viscoelastic effects would be minimized (Krishnan et al., 2004). The force was recorded at 20 Hz during testing and images were acquired from the top and the side at 2 Hz. A total of 58 samples were included in the data analysis, nine for each of the four groups and 24 for the dose–response study (described in Section 4.7).

4.4. Strain analysis

Images were acquired from the top and side cameras prior to testing to measure cross sectional area. The cameras were calibrated with a plastic blank, which had identical dimensions to the test sample. The strain was computed in the three principle directions using a custom Matlab program. The program tracked the strain along the test direction from the black micro beads, while strains along the width and thickness were determined by tracking the sample edges. For each frame, the center of the image corresponding to the test area was extracted and thresholded. An automated thresholding algorithm was used based on Otsu's method ('graythresh' function in Matlab) (D'Amore et al.). The thresholded image was segmented using the 'bwtraceboundary' function in Matlab. The edges of the gel were extracted from the images of the top and side by manual segmentation, and lines were fit to the edges. The differences between the center points of the best fit lines were taken to be the width or thickness of the sample. Changes in this distance were used to compute the engineering strain in these directions. The outlines of the beads were extracted from the thresholded image of the top video camera and a circle was fit to each bead. The centroids were then tracked to measure strain in the test direction (Lujan et al., 2007).

The cross sectional area in the reference configuration was computed from the reference width and thickness. The engineering stress was then computed for each sample by dividing the force by the reference area. Engineering stress was chosen as it is more commonly

Please cite this article as: Reese, S.P., et al., Effects of decorin proteoglycan on fibrillogenesis, ultrastructure, and mechanics of type I collagen gels, Matrix Biol. (2013), http://dx.doi.org/10.1016/j.matbio.2013.04.004

reported in the literature, thus allowing the direct comparison of stress–strain data (Roeder et al., 2002, 2009). The differential Poisson's ratio (Vader et al., 2009) was computed using $\nu_{ij} = -\frac{\partial e_i}{\partial e_j}$. The strain derivatives were found by fitting cubic splines to the strain data and then computing the derivatives of the splines relative to the sampling time. The Poisson's ratio was then computed using the chain rule: $\nu_{ij} = -\frac{\partial e_i}{\partial t}\left(\frac{\partial e_j}{\partial t}\right)^{-1}$. The derivative of the engineering stress–strain curve was computed using a window of ± 10 ten points in order to reduce errors due to noise. The maximal value for this derivative was taken to be the linear modulus of the sample, which typically occurred at ~20% clamp-to-clamp strain. The maximal stress attained during testing was taken to be the tensile strength. The modulus, tensile strength and maximal Poisson's ratios were compared between groups using a one way ANOVA (alpha = 0.05).

4.5. Microscopy

Immediately following mechanical testing the gels were fixed in 4% formaldehyde in PBS. Gels were prepared for scanning electron microscopy (SEM) analysis as previously described (Iwasaki et al., 2008). Gels were sputter coated with gold using a Pelco auto sputter coater (SC-7). Gels were imaged on an environmental SEM (Quanta 600 FEG, FEI, Hillsboro, OR) at high vacuum. Images were obtained at both 5000× and 15,000× for gels from 3 independent days of polymerization. Images were acquired at a resolution of 3775 × 4096 pixels. Six images were acquired of each sample at each magnification. A total of 18 images from three different days were acquired for each group at both magnifications. The images were examined qualitatively to determine the presence and density of fibrils, fibers and fiber bundles as defined in the previous literature that has studied collagen fibrillogenesis in vitro (Brightman et al., 2000; Mosser et al., 2006; Raub et al., 2007; Yang et al., 2009; Bailey et al., 2011) (Fig. 4).

For confocal reflection microscopy (CRM), gels were placed on a glass cover slip, kept moist with PBS and imaged using a 60× water lens at a wavelength of 488 nm. A total of 9 slices were imaged per stack using a 1 μm step size at a resolution of 2048 × 2048 pixels. Twelve samples were imaged, three from each group. All confocal microscopy was performed using an inverted Olympus FV1000. This confocal is fitted with a spectral version scan unit which allows for any emission wavelength or range to be studied. Images were captured between 488 and 489 nm.

4.6. Image analysis

An automated image analysis algorithm was used to extract the diameter of collagen structures within the gels (Pourdeyhimi et al., 1996; Pourdeyhimi and Dent, 1999; Stein et al., 2008; D'Amore et al.). The images were conditioned using a 3 × 3 median filter, a Gaussian smoothing filter (window = 6 pixels, standard deviation = 2 pixels) and histogram equalization (for SEM images only) to remove noise, increase contrast and smoothed the image (D'Amore et al.). Images were then thresholded using Otsu's method (D'Amore et al.). A skeletonization was performed on the binary image (bwmorph('skel') function in Matlab), followed by spur removal (bwmorph('spur') function in Matlab). The branch points of the skeleton were determined (bwmorph('branchoints') function in Matlab) and used as nucleation points for a direct tracking algorithm (Stein et al., 2008). The length of each collagen structure was determined as a line integral along the fiber. The width of each structure was determined by overlaying the skeleton on the distance transform of the black and white image (Pourdeyhimi and Dent, 1999). The area of each structure was determined by multiplying the average fiber width by the fiber length. This algorithm identified the diameter of structures in the thresholded image.

4.7. Dose–response study

Collagen gels were prepared with concentrations of 0, 1, 10, 25, 50 and 100 μg/mL of decorin (243, 24.3, 9.7, 4.9, and 2.4: 1 molar ratios of tropocollagen to decorin, respectively). A set of twelve gels were tested, with two samples for each concentration. Both the turbidity assay and mechanical testing were performed. Based on the results of this study, a concentration of 50 μg/mL was used for investigations described below unless stated otherwise. The small sample size for the dose–response study was due to the large amount of decorin required and the difficulty associated with the isolation of decorin. Because the sample size was inadequate for statistical comparison, the dose–response study was used for guiding the choice of decorin concentration only.

4.8. Decorin component study

To determine the part of the decorin proteoglycan that was responsible for altering collagen gel mechanics, collagen gels were prepared with 50 μg/mL decorin proteoglycan, decorin core protein, DS, or BSA as a control. Given the variability of the glycosaminoglycan side chain molecular weight, the concentration of decorin proteoglycan (50 μg/mL) is based on the protein core only. The absorption of decorin at 280 nm was used to determine its concentration, which does not include the mass contribution of the glycosaminoglycan. The molecular weights for decorin core protein, bovine serum albumin, and DS are 36,467 Da, 66,463 Da, and 30,000 Da respectively. Therefore the concentrations used in these experiments for decorin proteoglycan, decorin core protein, BSA, and DS equates to 1.37 μM, 1.37 μM, 0.75 μM, and 1.67 μM respectively. Decorin core protein was obtained by treating 350 μL of decorin (0.6 mg/mL) with 0.02 units of chondoitinase ABC (Sigma) at 37 °C overnight. Dermatan sulfate purified from porcine intestinal mucosa was obtained from EMD chemicals. The turbidity assay, material testing, and microscopy were performed as described in the previous method sections.

4.9. Effects of temperature

To determine if decorin had the same effect at higher polymerization temperatures, gels were polymerized with and without decorin at 37 °C. A total of three gels were polymerized for the control and decorin gels at 37 °C. After the completion of polymerization, gels were subjected to the material test protocol described in Sections 4.2–4.6.

4.10. Post-polymerization addition of decorin

To test whether decorin must be present during polymerization in order to affect the material properties of collagen gels, three groups of gels were tested: control gels (without decorin), gels with 70 μg/mL decorin added prior to polymerization and gels with decorin added 1 h after the initiation of polymerization. All gels were poured into the molds at room temperature (RT) and allowed to polymerize for 1 h, at which point 125 μL of PBS was applied to the surface (test area) of the control and decorin containing gels. The third set of gels had 125 μL of decorin containing PBS (87.5 μg total decorin) applied to the test area surface. Gels were then incubated at 37 °C to facilitate diffusion of the decorin into the gels. To verify that decorin had penetrated into the test area of the gels, an extra set of gels not used for testing was stained with dimethyl methyl blue, which changes color from blue to pink as it binds to glycosaminoglycans (Kiraly et al., 1996). Prior to staining, the gels were each washed in 50 mL of PBS. A total of 6 gels were subjected to material testing for each group.

Please cite this article as: Reese, S.P., et al., Effects of decorin proteoglycan on fibrillogenesis, ultrastructure, and mechanics of type I collagen gels, Matrix Biol. (2013), http://dx.doi.org/10.1016/j.matbio.2013.04.004

Acknowledgments

Financial support from NIH grant #R01AR047369 is gratefully acknowledged.

Appendix A. Supplementary data

Supplementary data to this article can be found online at http://dx.doi.org/10.1016/j.matbio.2013.04.004.

References

Ateshian, G.A., Rajan, V., Chahine, N.O., Canal, C.E., Hung, C.T., 2009. Modeling the matrix of articular cartilage using a continuous fiber angular distribution predicts many observed phenomena. J. Biomech. Eng. 131, 061003.

Bailey, J.L., Critser, P.J., Whittington, C., Kuske, J.L., Yoder, M.C., Voytik-Harbin, S.L., 2011. Collagen oligomers modulate physical and biological properties of three-dimensional self-assembled matrices. Biopolymers 95, 77–93.

Banos, C.C., Thomas, A.H., Kuo, C.K., 2008. Collagen fibrillogenesis in tendon development: current models and regulation of fibril assembly. Birth Defects Res. C Embryo Today 84, 228–244.

Barocas, V.H., Tranquillo, R.T., 1997. A finite element solution for the anisotropic biphasic theory of tissue-equivalent mechanics: the effect of contact guidance on isometric cell traction measurement. J. Biomech. Eng. 119, 261–268.

Birk, D.E., Southern, J.F., Zycband, E.I., Fallon, J.T., Trelstad, R.L., 1989. Collagen fibril bundles: a branching assembly unit in tendon morphogenesis. Development 107, 437–443.

Birk, D.E., Fitch, J.M., Babiarz, J.P., Doane, K.J., Linsenmayer, T.F., 1990. Collagen fibrillogenesis in vitro: interaction of types I and V collagen regulates fibril diameter. J. Cell Sci. 95 (Pt 4), 649–657.

Birk, D.E., Zycband, E.I., Woodruff, S., Winkelmann, D.A., Trelstad, R.L., 1997. Collagen fibrillogenesis in situ: fibril segments become long fibrils as the developing tendon matures. Dev. Dyn. 208, 291–298.

Brightman, A.O., Rajwa, B.P., Sturgis, J.E., McCallister, M.E., Robinson, J.P., Voytik-Harbin, S.L., 2000. Time-lapse confocal reflection microscopy of collagen fibrillogenesis and extracellular matrix assembly in vitro. Biopolymers 54, 222–234.

Brown, D.C., Vogel, K.G., 1989. Characteristics of the in vitro interaction of a small proteoglycan (PG II) of bovine tendon with type I collagen. Matrix 9, 468–478.

Chandran, P.L., Barocas, V.H., 2007. Deterministic material-based averaging theory model of collagen gel micromechanics. J. Biomech. Eng. 129, 137–147.

Cheema, U., Chuo, C.B., Sarathchandra, P., Nazhar, N.S., Brown, R.A., 2007. Engineering functional collagen scaffolds: cyclical loading increases material strength and fibril aggregation. Adv. Funct. Mater. 17, 2426–2431.

Craig, A.S., Birtles, M.J., Conway, J.F., Parry, D.A., 1989. An estimate of the mean length of collagen fibrils in rat tail-tendon as a function of age. Connect. Tissue Res. 19, 51–62.

D'Amore, A., Stella, J.A., Wagner, W.R., Sacks, M.S., 2010. Characterization of the complete fiber network topology of planar fibrous tissues and scaffolds. Biomaterials 31, 5345–5354.

Danielson, K.G., Baribault, H., Holmes, D.F., Graham, H., Kadler, K.E., Iozzo, R.V., 1997. Targeted disruption of decorin leads to abnormal collagen fibril morphology and skin fragility. J. Cell Biol. 136, 729–743.

Douglas, T., Heinemann, S., Bierbaum, S., Scharnweber, D., Worch, H., 2006. Fibrillogenesis of collagen types I, II, and III with small leucine-rich proteoglycans decorin and biglycan. Biomacromolecules 7, 2388–2393.

Elliott, D.M., Robinson, P.S., Gimbel, J.A., Sarver, J.J., Abboud, J.A., Iozzo, R.V., Soslowsky, L.J., 2003. Effect of altered matrix proteins on quasilinear viscoelastic properties in transgenic mouse tail tendons. Ann. Biomed. Eng. 31, 599–605.

Farndale, R.W., Buttle, D.J., Barrett, A.J., 1986. Improved quantitation and discrimination of sulphated glycosaminoglycans by use of dimethylmethylene blue. Biochim. Biophys. Acta 883, 173–177.

Fleischmajer, R., Fisher, L.W., MacDonald, E.D., Jacobs Jr., L., Perlish, J.S., Termine, J.D., 1991. Decorin interacts with fibrillar collagen of embryonic and adult human skin. J. Struct. Biol. 106, 82–90.

Goldoni, S., Owens, R.T., McQuillan, D.J., Shriver, Z., Sasisekharan, R., Birk, D.E., Campbell, S., Iozzo, R.V., 2004. Biologically active decorin is a monomer in solution. J. Biol. Chem. 279, 6606–6612.

Hassell, J.R., Birk, D.E., 2010. The molecular basis of corneal transparency. Exp. Eye Res. 91, 326–335.

Hedbom, E., Heinegard, D., 1989. Interaction of a 59-kDa connective tissue matrix protein with collagen I and collagen II. J. Biol. Chem. 264, 6898–6905.

Hedbom, E., Heinegard, D., 1993. Binding of fibromodulin and decorin to separate sites on fibrillar collagens. J. Biol. Chem. 268, 27307–27312.

Iwasaki, S., Hosaka, Y., Iwasaki, T., Yamamoto, K., Nagayasu, A., Ueda, H., Kokai, Y., Takehana, K., 2008. The modulation of collagen fibril assembly and its structure by decorin: an electron microscopic study. Arch. Histol. Cytol. 71, 37–44.

Kadler, K.E., Hill, A., Canty-Laird, E.G., 2008. Collagen fibrillogenesis: fibronectin, integrins, and minor collagens as organizers and nucleators. Curr. Opin. Cell Biol. 20, 495–501.

Kalamajski, S., Oldberg, A., 2010. The role of small leucine-rich proteoglycans in collagen fibrillogenesis. Matrix Biol. 29, 248–253.

Kaya, M., Toyama, Y., Kubota, K., Nodasaka, Y., Ochiai, M., Nomizu, M., Nishi, N., 2005. Effect of DNA structure on the formation of collagen–DNA complex. Int. J. Biol. Macromol. 35, 39–46.

Kiraly, K., Lapvetelainen, T., Arokoski, J., Torronen, K., Modis, L., Kiviranta, I., Helminen, H.J., 1996. Application of selected cationic dyes for the semiquantitative estimation of glycosaminoglycans in histological sections of articular cartilage by microspectrophotometry. Histochem. J. 28, 577–590.

Kishore, V., Paderi, J.E., Akkus, A., Smith, K.M., Balachandran, D., Beaudoin, S., Panitch, A., Akkus, O., 2011. Incorporation of a decorin biomimetic enhances the mechanical properties of electrochemically aligned collagen threads. Acta Biomater. 7, 2428–2436.

Kjaer, M., 2004. Role of extracellular matrix in adaptation of tendon and skeletal muscle to mechanical loading. Physiol. Rev. 84, 649–698.

Krishnan, L., Weiss, J.A., Wessman, M.D., Hoying, J.B., 2004. Design and application of a test system for viscoelastic characterization of collagen gels. Tissue Eng. 10, 241–252.

Kuc, I.M., Scott, P.G., 1997. Increased diameters of collagen fibrils precipitated in vitro in the presence of decorin from various connective tissues. Connect. Tissue Res. 36, 287–296.

Lujan, T.J., Underwood, C.J., Henninger, H.B., Thompson, B.M., Weiss, J.A., 2007. Effect of dermatan sulfate glycosaminoglycans on the quasi-static material properties of the human medial collateral ligament. J. Orthop. Res. 25, 894–903.

Lujan, T.J., Underwood, C.J., Jacobs, N.T., Weiss, J.A., 2009. Contribution of glycosaminoglycans to viscoelastic tensile behavior of human ligament. J. Appl. Physiol. 106, 423–431.

Mosser, G., Anglo, A., Helary, C., Bouligand, Y., Giraud-Guille, M.M., 2006. Dense tissue-like collagen matrices formed in cell-free conditions. Matrix Biol. 25, 3–13.

Orgel, J.P., Irving, T.C., Miller, A., Wess, T.J., 2006. Microfibrillar structure of type I collagen in situ. Proc. Natl. Acad. Sci. U. S. A. 103, 9001–9005.

Pins, G.D., Christiansen, D.L., Patel, R., Silver, F.H., 1997. Self-assembly of collagen fibers. Influence of fibrillar alignment and decorin on mechanical properties. Biophys. J. 73, 2164–2172.

Pourdeyhimi, B., Dent, R., 1999. Measuring fiber diameter distribution in nonwovens. Text. Res. J. 69, 233–236.

Pourdeyhimi, B., Ramanathan, R., Dent, R., 1996. Measuring fiber orientation in nonwovens. Part II: direct tracking. Text. Res. J. 66, 747–753.

Pringle, G.A., Dodd, C.M., 1990. Immunoelectron microscopic localization of the core protein of decorin near the d and e bands of tendon collagen fibrils by use of monoclonal antibodies. J. Histochem. Cytochem. 38, 1405–1411.

Provenzano, P.P., Heisey, D., Hayashi, K., Lakes, R., Vanderby Jr., R., 2002. Subfailure damage in ligament: a structural and cellular evaluation. J. Appl. Physiol. 92, 362–371.

Rada, J.A., Cornuet, P.K., Hassell, J.R., 1993. Regulation of corneal collagen fibrillogenesis in vitro by corneal proteoglycan (lumican and decorin) core proteins. Exp. Eye Res. 56, 635–648.

Raspanti, M., Viola, M., Sonaggere, M., Tira, M.E., Tenni, R., 2007. Collagen fibril structure is affected by collagen concentration and decorin. Biomacromolecules 8, 2087–2091.

Raspanti, M., Viola, M., Forlino, A., Tenni, R., Gruppi, C., Tira, M.E., 2008. Glycosaminoglycans show a specific periodic interaction with type I collagen fibrils. J. Struct. Biol. 164, 134–139.

Raub, C.B., Suresh, V., Krasieva, T., Lyubovitsky, J., Mih, J.D., Putnam, A.J., Tromberg, B.J., George, S.C., 2007. Noninvasive assessment of collagen gel microstructure and mechanics using multiphoton microscopy. Biophys. J. 92, 2212–2222.

Robinson, P.S., Lin, T.W., Jawad, A.F., Iozzo, R.V., Soslowsky, L.J., 2004a. Investigating tendon fascicle structure–function relationships in a transgenic-age mouse model using multiple regression models. Ann. Biomed. Eng. 32, 924–931.

Robinson, P.S., Lin, T.W., Reynolds, P.R., Derwin, K.A., Iozzo, R.V., Soslowsky, L.J., 2004b. Strain-rate sensitive mechanical properties of tendon fascicles from mice with genetically engineered alterations in collagen and decorin. J. Biomech. Eng. 126, 252–257.

Robinson, P.S., Huang, T.F., Kazam, E., Iozzo, R.V., Birk, D.E., Soslowsky, L.J., 2005. Influence of decorin and biglycan on mechanical properties of multiple tendons in knockout mice. J. Biomech. Eng. 127, 181–185.

Roeder, B.A., Kokini, K., Sturgis, J.E., Robinson, J.P., Voytik-Harbin, S.L., 2002. Tensile mechanical properties of three-dimensional type I collagen extracellular matrices with varied microstructure. J. Biomech. Eng. 124, 214–222.

Roeder, B.A., Kokini, K., Voytik-Harbin, S.L., 2009. Fibril microstructure affects strain transmission within collagen extracellular matrices. J. Biomech. Eng. 131, 031004.

Ruhland, C., Schonherr, E., Robenek, H., Hansen, U., Iozzo, R.V., Bruckner, P., Seidler, D.G., 2007. The glycosaminoglycan chain of decorin plays an important role in collagen fibril formation at the early stages of fibrillogenesis. FEBS J. 274, 4246–4255.

Sander, E.A., Stylianopoulos, T., Tranquillo, R.T., Barocas, V.H., 2009a. Image-based biomechanics of collagen-based tissue equivalents. IEEE Eng. Med. Biol. Mag. 28, 10–18.

Sander, E.A., Stylianopoulos, T., Tranquillo, R.T., Barocas, V.H., 2009b. Image-based multiscale modeling predicts tissue-level and network-level fiber reorganization in stretched cell-compacted collagen gels. Proc. Natl. Acad. Sci. U. S. A. 106, 17675–17680.

Schonherr, E., Hausser, H., Beavan, L., Kresse, H., 1995. Decorin-type I collagen interaction. Presence of separate core protein-binding domains. J. Biol. Chem. 270, 8877–8883.

Scott, J.E., 1988. Proteoglycan–fibrillar collagen interactions. Biochem. J. 252, 313–323.

Scott, J.E., 1996. Proteodermatan and proteokeratan sulfate (decorin, lumican/fibromodulin) proteins are horseshoe shaped. Implications for their interactions with collagen. Biochemistry 35, 8795–8799.

Scott, J.E., 2003. Elasticity in extracellular matrix 'shape modules' of tendon, cartilage, etc. A sliding proteoglycan-filament model. J. Physiol. 553, 335–343.

Scott, J.E., Orford, C.R., 1981. Dermatan sulphate-rich proteoglycan associates with rat tail-tendon collagen at the d band in the gap region. Biochem. J. 197, 213–216.

Scott, J.E., Thomlinson, A.M., 1998. The structure of interfibrillar proteoglycan bridges ('shape modules') in extracellular matrix of fibrous connective tissues and their stability in various chemical environments. J. Anat. 192 (Pt 3), 391–405.

Please cite this article as: Reese, S.P., et al., Effects of decorin proteoglycan on fibrillogenesis, ultrastructure, and mechanics of type I collagen gels, Matrix Biol. (2013), http://dx.doi.org/10.1016/j.matbio.2013.04.004

Scott, J.E., Orford, C.R., Hughes, E.W., 1981. Proteoglycan–collagen arrangements in developing rat tail tendon. An electron microscopical and biochemical investigation. Biochem. J. 195, 573–581.
Scott, P.G., McEwan, P.A., Dodd, C.M., Bergmann, E.M., Bishop, P.N., Bella, J., 2004. Crystal structure of the dimeric protein core of decorin, the archetypal small leucine-rich repeat proteoglycan. Proc. Natl. Acad. Sci. U. S. A. 101, 15633–15638.
Shi, J.H., Liu, X.Y., Li, L.J., Strom, C.S., Xu, H.Y., 2009. Spherulitic networks: from structure to rheological property. J. Phys. Chem. B 113, 4549–4554.
Silver, F.H., Freeman, J.W., Seehra, G.P., 2003. Collagen self-assembly and the development of tendon mechanical properties. J. Biomech. 36, 1529–1553.
Stein, A.M., Vader, D.A., Jawerth, L.M., Weitz, D.A., Sander, L.M., 2008. An algorithm for extracting the network geometry of three-dimensional collagen gels. J. Microsc. 232, 463–475.
Svensson, L., Aszodi, A., Reinholt, F.P., Fassler, R., Heinegard, D., Oldberg, A., 1999. Fibromodulin-null mice have abnormal collagen fibrils, tissue organization, and altered lumican deposition in tendon. J. Biol. Chem. 274, 9636–9647.
Tatlier, M., Berhan, L., 2009. Modelling the negative poisson's ratio of compressed fused fibre networks. Phys. Status Solidi B 246, 2018–2024.
Uldbjerg, N., Danielsen, C.C., 1988. A study of the interaction in vitro between type I collagen and a small dermatan sulphate proteoglycan. Biochem. J. 251, 643–648.
Vader, D., Kabla, A., Weitz, D., Mahadevan, L., 2009. Strain-induced alignment in collagen gels. PLoS One 4, e5902.
Vogel, K.G., Trotter, J.A., 1987. The effect of proteoglycans on the morphology of collagen fibrils formed in vitro. Coll. Relat. Res. 7, 105–114.
Vogel, K.G., Paulsson, M., Heinegard, D., 1984. Specific inhibition of type I and type II collagen fibrillogenesis by the small proteoglycan of tendon. Biochem. J. 223, 587–597.
Weber, I.T., Harrison, R.W., Iozzo, R.V., 1996. Model structure of decorin and implications for collagen fibrillogenesis. J. Biol. Chem. 271, 31767–31770.
Wenstrup, R.J., Smith, S.M., Florer, J.B., Zhang, G., Beason, D.P., Seegmiller, R.E., Soslowsky, L.J., Birk, D.E., 2011. Regulation of collagen fibril nucleation and initial fibril assembly involves coordinate interactions with collagens V and XI in developing tendon. J. Biol. Chem. 286, 20455–20465.
Yang, Y.L., Leone, L.M., Kaufman, L.J., 2009. Elastic moduli of collagen gels can be predicted from two-dimensional confocal microscopy. Biophys. J. 97, 2051–2060.
Zhang, G., Young, B.B., Ezura, Y., Favata, M., Soslowsky, L.J., Chakravarti, S., Birk, D.E., 2005. Development of tendon structure and function: regulation of collagen fibrillogenesis. J. Musculoskelet. Neuronal. Interact. 5, 5–21.
Zhang, G., Ezura, Y., Chervoneva, I., Robinson, P.S., Beason, D.P., Carine, E.T., Soslowsky, L.J., Iozzo, R.V., Birk, D.E., 2006. Decorin regulates assembly of collagen fibrils and acquisition of biomechanical properties during tendon development. J. Cell. Biochem. 98, 1436–1449.
Zhang, G., Chen, S., Goldoni, S., Calder, B.W., Simpson, H.C., Owens, R.T., McQuillan, D.J., Young, M.F., Iozzo, R.V., Birk, D.E., 2009. Genetic evidence for the coordinated regulation of collagen fibrillogenesis in the cornea by decorin and biglycan. J. Biol. Chem. 284, 8888–8897.

Please cite this article as: Reese, S.P., et al., Effects of decorin proteoglycan on fibrillogenesis, ultrastructure, and mechanics of type I collagen gels, Matrix Biol. (2013), http://dx.doi.org/10.1016/j.matbio.2013.04.004